

Supplemental Experimental Procedures

Animals and diets

For all experiments, mice were housed in a ventilated rack with ad libitum access to food and water under a 12hr light/dark schedule (lights-on at 6:00AM). Mice were genotyped using a commercial service (Transnetyx) with randomly selected tails from each litter validated using the recommended primer sequences from Jackson Labs. For the IL1R1flox (IL1R1^{fl/fl}) line, genomic DNA amplification was carried out as recommended by the donating investigator (34). For VAT transplantation, recipient mice were bred in-house and maintained on LFD (Research Diets D12450) or normal chow (Teklad) before surgery at 12wk old. CX3CR1^{creER}/IL1R1^{fl/fl} transgenic recipients and nontransgenic male littermates received tamoxifen one month before surgery. Mice were randomly assigned to receive IPGTT or cognitive testing before being euthanized for cell isolation, slice preparation, or tissue collection.

Adipose tissue transplantation and determination of transplant viability

For WAT transplantation, the epididymal (VAT) or inguinal (SAT) fat pads were removed from HFD donors and trimmed to 300mg before transplantation into the peritoneal cavity of recipients, as reported previously (75). Parallel groups of mice received sham surgery. Transplants were collected at euthanasia for histological verification of transplant viability, as described (75). In brief, montage images of HNE staining across the entire transplant were acquired through a 10X objective on a microscope with a motorized stage using Microlucida software (Microbrightfield, Williston, VT USA). Brightfield montages were converted to grayscale and thresholded algorithmically in ImageJ software (freely available at <https://imagej.nih.gov/ij/>). The total area of dead tissue was quantified relative to total transplant area, excluding the ten microns around the border where transplants were trimmed to generate uniform sizes at the time of surgery. Transplants with <10% dead tissue were considered viable and mice with >10% dead tissue were excluded from experimental datasets.

Enzyme-linked immunosorbent assay and western blotting

Interleukin-1 β was measured in protein lysates and serum using a commercially available kit (R&D Systems). Concentrations were expressed relative to total protein, as determined by Bradford assay (Bio-Rad). Protein extraction from hippocampus and adipose tissue was carried out as reported previously (28, 75). For the ex vivo stimulation experiments, levels of TNF α in cell supernatants were also determined using a commercially available kit (R&D Systems), as described (79). For detection of 6x-Histidine by western blotting, lysates (10 μ g/lane) were separated on 4-12% gradient gels by SDS-PAGE and transferred to nitrocellulose membranes (0.45 μ m pore size). After blocking in 5% BSA, membranes were incubated with rabbit anti-6xHis (Abcam, catalog #ab9108) and mouse anti-beta actin (Sigma-Aldrich, catalog #A5441). Primary antibody incubation was followed by washes and detection with NIR-conjugated secondary antibodies. Membranes were imaged on a Li-Cor Odyssey instrument and quantified in ImageStudio version 5 (Li-Cor).

Immunofluorescence, confocal microscopy, and morphological analysis

For immunofluorescence and peroxidase histochemistry, 40 μ m coronal sections were cut throughout the rostrocaudal extent of the hippocampus as a 1:6 series using a freezing microtome (Leica). Sections were stored at -20 $^{\circ}$ C in cryoprotectant before being processed for IBA1/MHCII or IBA1/CD68 double-labeling. Immunoperoxidase detection and stereological quantification of IBA1 was carried out as described (26). For immunofluorescence, sections were washed in Tris-buffered saline (TBS), blocked, and reacted overnight at 4C with rabbit polyclonal anti-IBA1 (Wako, catalog #019-19741), mouse monoclonal anti-MHCII (AbDSerotec, catalog #MCA46G), and/or rat anti-CD68 (AbDSerotec, catalog #MCA1957). After primary antibody incubation, sections were washed in TBS and reacted with fluorophore-conjugated secondary antibodies (Invitrogen, Carlsbad, CA) before being mounted on Superfrost Plus slides. Slides were counterstained with DAPI before imaging on a Zeiss 780 multiphoton microscope and blind analysis. For analysis of MHCII, (50) z-stack images of IBA1+ cells were acquired from the dentate molecular layer and colocalization was evaluated by a blind experimenter. For analysis of CD68, the area of punctate labeling within regions of

interest (ROIs) defined by IBA1+ cells was determined as shown in Supplemental Figure 1A-B and as previously reported for other antigens (28). Microglia were also traced in a semi-automated manner on (10-12) cells per animal using Neurolucida 360 (Microbrightfield, VT USA). Total process lengths and the number of intersections at 1-micron intervals around the soma were averaged on a per-animal basis and used for subsequent statistical comparisons.

For measures of dendritic spine density, image stacks were acquired at 0.1 micron step size for semiautomated spine detection and classification in Neurolucida 360. After manual validation of detected spines, images were exported as serial tiffs for analysis of colocalization between IBA1+ microglial processes and GFP+ dendrites in Fiji software (freely available at <https://fiji.sc>). Serial z-stack images of colocalized points were exported in .tif format and imported into the NL360 datafile containing detected and classified spine tracings. Colocalized points that overlapped with dendritic spines in the NL360 datafile were manually identified using different markers for thin, stubby, and mushroom spines. The density of spines that colocalized with IBA1+ processes was expressed relative to total spine density on a per-animal basis for statistical comparisons.

Cell isolation and ex vivo stimulation

Forebrain mononuclear cells (FMCs), astrocytes, and BVECs were isolated according to published protocols (28). In brief, astrocytes and FMCs were separated on a discontinuous gradient of isotonic Percoll at the following concentrations: 75%, 50%, 30%, 0%. Microglia were collected from the 75%/50% interphase, astrocytes were collected from the 50%/30% interphase, and glia-depleted brain tissue from the 30%/0% interphase was collected for qPCR analysis of separation efficacy (see section on gene expression endpoints). For isolation of BVECs, the cerebellum and midline white matter were discarded and hemispheres were manually dissociated in vascular isolation buffer (VIB; 28) using a Tenbroeck homogenizer. After brief centrifugation, dissociated cells were resuspended in VIB and layered on top of an equal volume of 15% dextran. Dextran gradients were separated by centrifugation at 1,500xg for 1hr at 4C in a swinging bucket rotor. After separation, the vascular pellet under the dextran layer was washed by resuspension in VIB and the vascular-depleted brain tissue was collected from the

VIB/dextran interphase for qPCR validation of separation efficacy. After centrifugation, the vascular pellet was resuspended in VIB with 2% heat-inactivated FBS and passed through a 100-micron cell strainer. The flow-through was then passed through a 40-micron cell strainer, which was immediately transferred to a 6-well plate containing VIB+2%FBS for microvessel collection. Cell pellets were frozen for gene expression endpoints or processed for antibody labeling and flow cytometry.

For ex vivo stimulation, FMCs were isolated as described for flow cytometry and qPCR endpoints. Cell viability and yield were determined immediately after isolation by ViaCount assay (MilliporeSigma). Cells were plated in v-bottom 96-well plates (10^5 cells/well) and adhered for 1hr in serum-free DMEM at 37C under 5%CO₂, as reported previously (75, 79). After adherence, media was aspirated from each well and replaced with DMEM containing 10%FBS and recombinant murine IL1 β (0, 0.25, 0.5, or 1.0ng/mL; Shenandoah Biotechnologies). Cells were stimulated for 16hr before collecting media samples for analysis of TNF α . Media was exchanged for an equal volume of reagents from a colorimetric viability kit (R&D Systems catalog #4891-025-K). The viability assay was carried out for 30min according to the manufacturer's instructions and as described (75, 79). After incubation, assay reagents were transferred to a standard 96-well plate and optical densities were read at 490nm and 630nm on a SpectraMax Abs plate reader (Molecular Devices, Carlsbad, CA). Optical densities from cells stimulated with 0.25, 0.5, or 1.0ng/mL IL1 β were expressed relative to the unstimulated well for analysis of viability. Cells were collected from the original v-bottom plate, snap frozen, and stored at -80C in preparation for RNA extraction and qPCR.

Flow cytometry

For cell-surface markers, immunophenotyping was carried out in forebrain mononuclear cells (FMCs) as described (29). In brief, cells from the 70%/50% interphase were washed and resuspended in Dulbecco's phosphate-buffered saline (dPBS) with 10% heat-inactivated fetal bovine serum (dPBS+FBS). For immunodetection, cells (5×10^4 cells/100uL) were blocked in dPBS+FBS for 30min before incubation with antibodies against CD11b (AbDSerotec, clone M1/70.15), CD45 (AbDSerotec, clone YW62.3), and Ly6-C (Biolegend, clone HK1.4). For analysis of activation markers, cells were labeled

with antibodies against CD11b, MHCII (AbDSerotec, clone OX-6) and TLR4 (Biolegend, clone MTS510). Cell-surface expression of IL1R1 in myeloid lineage cells was detected using a monoclonal IL1R1 antibody (clone 129304; R&D Systems). Acquisition thresholds were determined using unlabeled cells and isotype controls. Compensation parameters were generated from single-channel acquisition of PE-Cy5, PE, and FITC-conjugated antibodies or stains. For each label or combination of labels, 1×10^4 events were acquired using a BD FACSCalibur or Guava EasyCyte 5 flow cytometer. Cells were gated on forward and side scatter and dead cells were excluded based on DAPI, 7AAD, or Sytox Orange fluorescence. Expression of phenotypic and activation markers was determined within the SSC_{low}/FSC_{mid}/CD11b⁺ population, as described (29).

For intracellular flow cytometry, live cells were incubated with conjugated antibodies against CD45, Ly6C, and CD11b. Following a PBS wash, cells were fixed and permeabilized using Fixation/Permeabilization Concentrate (Affymetrix eBioscience) and then incubated with antibodies for intracellular labeling of IL1 β . After a final wash, cells were analyzed using a four-laser BD LSRII flow cytometer (BD Biosciences). Isotype-matched controls were analyzed to set the appropriate gates for each sample. Viable cells were visibly differentiated from debris by gating on live cells with high forward scatter (FSC) and positivity for specific antibodies. Single stains were performed for compensation controls, controls to check for fluorescence spread, and isotype controls were used to determine the level of nonspecific binding. Cells expressing a specific marker were reported as a percentage of the number of gated events. Analysis was carried out in FlowJo version 11.0 (BD Bioscience) or InCyte software (Millipore, Temecula, CA).

RNA isolation and qPCR

Total RNA extraction from primary cell populations and whole hippocampus followed previously published methodology (28, 64). In brief, RNA samples were extracted and column-purified using RNeasy system (Qiagen). cDNA was synthesized from the purified RNA template using a commercially available kit (Applied Biosystems). For qPCR, 500ng cDNA was amplified using Applied Biosystems 2xMastermix and Taqman probes on a StepOne plus instrument. Expression was determined by calculating

the ddCT, with average dCT for nTg/LFD samples as the reference group in each cell type. In the IL1 β -stimulated gene expression studies, the average dCT for cDNA samples from unstimulated LFD/SHAM microglia was used as the reference group. The following Taqman probes were used in these experiments: IL1 β , Mm00434228_m1; IL1R1, Mm00434237_m1; IL6, Mm00446190_m1; MCP1/CCL2, Mm00441242_m1; TLR4, Mm00445273_m1; Gapdh, Mm99999915_g1.

For routine quality control, cell type-specific genes were amplified from FMCs, astrocytes, microvessels, and control interphases using the following primers in SybrGreen mastermix: CD11b (F:5'-TGGATTGATGCAGAAATGTG-3'; R:5'-TGAAGAACCTCTGAGCATCC-3'); Fcrls (F: 5'-GGCTCCTATTCCTGTAAGGC-3'; R:5'-ACAGCTCTTGGACATTCAGC-3'); Gfap (F:5'-AACAACTGGCTGCGTATAG-3'; R:5'-GGAGTTCTCGAACTTCCTCC-3'); Glast1 (F:5'-TGGCCAAGAAGAAAGTTCAG-3'; R:5'-TGTACCCACAATGACAGCAG-3'); Tie2 (F:5'-CTTGGACAATAGTGGATGGC-3'; R:5'-TTCACATCAATGTGCTGGTC-3'); Cdh5 (F:5'-CACTGCTTTGGGAGCCTTC-3'; R:5'-GGGGCAGCGATTCATTTTTTCT-3'); and Gapdh (F:5'-GGGAAGCCCATCACCATCTT-3'; R:5'-GCCTCACCCATTTGATGTT-3'). Expression of phenotypic genes was compared across different cell types isolated from the same animal and only samples with at least threefold greater enrichment in the appropriate population were used for subsequent analysis. Routine validation reactions for qPCR were assembled using an epMotion 5073 robotic pipettor (Eppendorf).

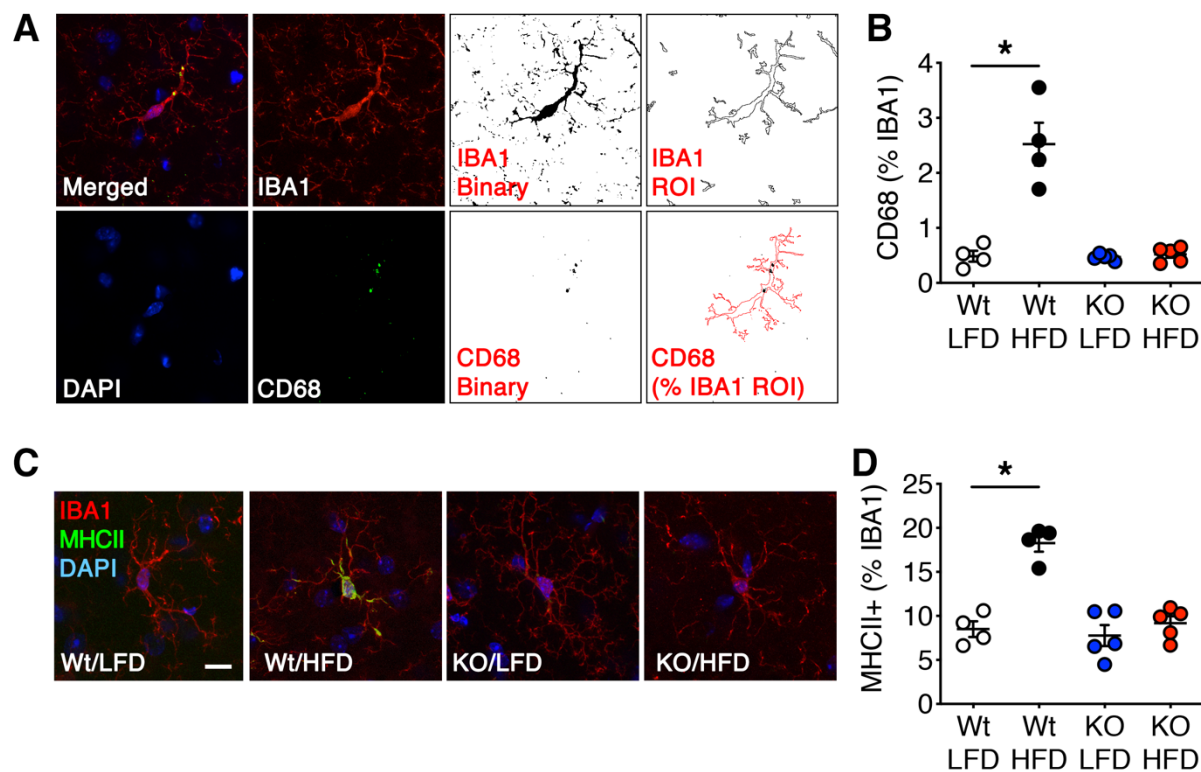
Total RNA was also extracted from a subset of paraffin-embedded transplants for cDNA synthesis and qPCR. For RNA extraction, four 2mm tissue punches were taken from each block and transferred to a tube containing 1mL Citrisolv. Samples were heated in Citrisolv at 55°C for 30min to remove paraffin before centrifugation at 13,000rpm for 10min to pellet tissue. After removal of supernatant, the pellet was washed twice with 100% ETOH before being transferred to a vacuum dryer for 15min. The pellet was rehydrated and dissociated in a bead-blaster for 3min before protein digestion and de-crosslinking (2hr at 55C, then 1hr at 88C). After protein digestion, genomic DNA was digested in the presence of DNase for 30min at 37C before RNA isolation. RNA was isolated after digestion by column purification using the RNeasy kit (Qiagen). RNA was eluted in 60uL Nuclease Free water and concentrations were read on a NanoDrop

instrument (Thermo Fisher). For reverse transcription, 500ng RNA was reverse transcribed using random primers (part# 4368813) with a High Capacity cDNA Reverse Transcription kit (40uL reaction vol; Thermo Fisher). Real-time PCR reactions were then carried out using Taqman probes and Taqman Mastermix (Applied Biosystems).

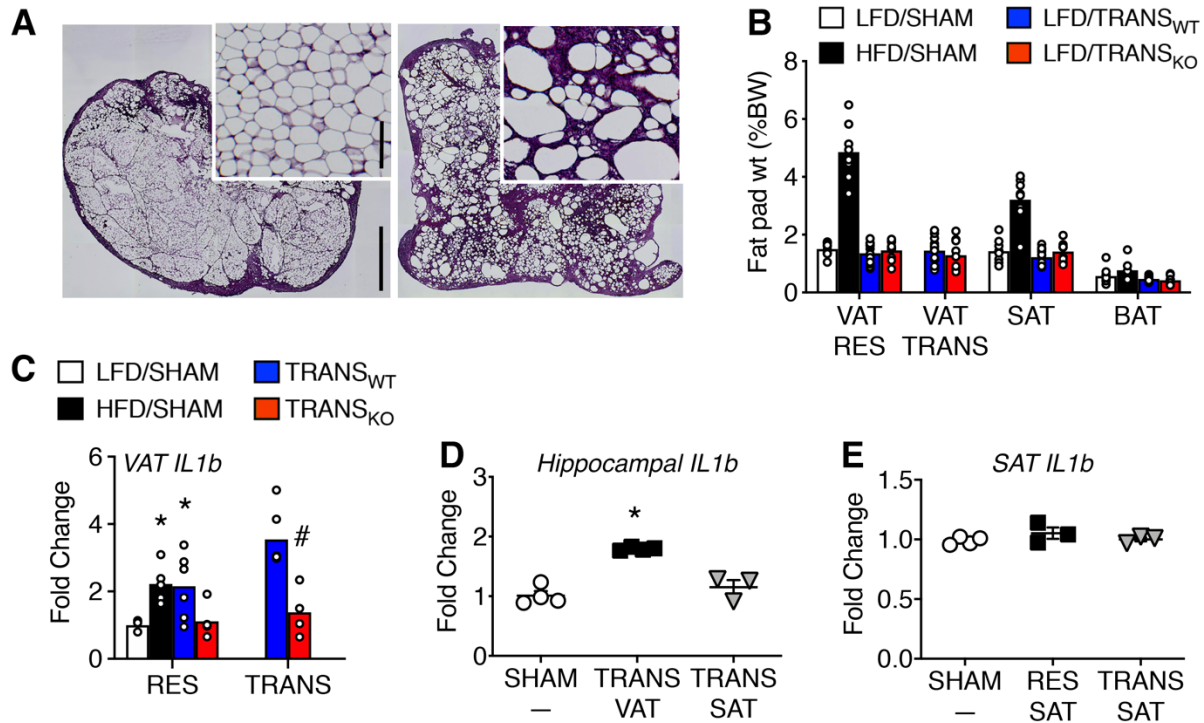
Hippocampal slice preparation and electrophysiology

Methods for hippocampal slice preparation and extracellular recording of dentate gyrus LTP were published previously (28-29, 75). In brief, baseline recordings were acquired at 0.05Hz and LTP was induced using a single 1-second train delivered at 100Hz. For some experiments, slices were pre-incubated in ACSF with 100 ug/mL recombinant IL1RA for 20min, with continuous bath application of IL1RA throughout recording to block IL1 receptor activation. In other experiments, slices were incubated with recombinant murine IL1 β (1.0ng/mL) for 20min before recording, with continuous superfusion of IL1 β throughout recording. A subset of slices from the IL1 β experiments were pre-incubated with minocycline (20 μ M) for 30min before concurrent exposure to IL1 β and minocycline throughout recording. LTP magnitude was determined by calculating the percent increase in field excitatory postsynaptic potential (fEPSP) slope during minutes 50-60 after induction, relative to pre-induction baseline, as described (28-29, 75).

Supplemental Figures



Supplemental Figure 1. Dietary obesity elicits NLRP3-mediated microglial activation in the hippocampal dentate gyrus. (A) Method for quantification of CD68+ puncta within regions of interest (ROIs) defined by IBA1+ microglia. (B) Dietary obesity promotes microglial CD68 accumulation via NLRP3. (C) Immunofluorescence visualization of the classical activation marker MHCII among hippocampal microglia. (D) Obesity-induced MHCII expression requires NLRP3. For all graphs, line height represents the mean and error bars represent SEM. Asterisk (*) denotes statistical significance at $p < 0.05$ by 2-way ANOVA with Tukey's post hoc.

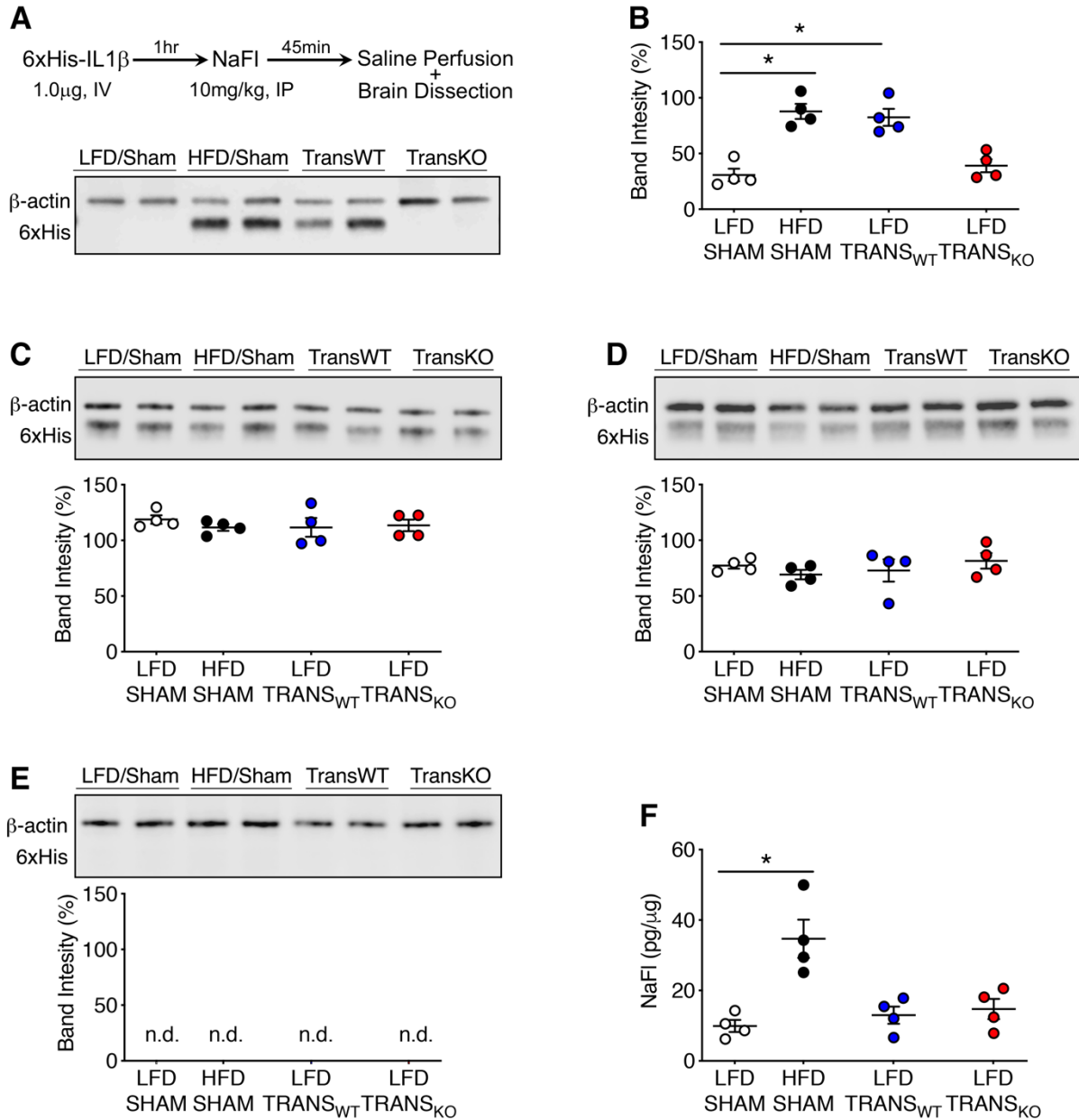


Supplemental Figure 2. Transplant viability and depot-specific regulation of IL1 β .

(A) Representative histological image of HNE staining in a healthy transplant (left; scale bar = 2.5mm; for inset, scale bar = 0.1mm) and a rejected transplant (right; same scale).

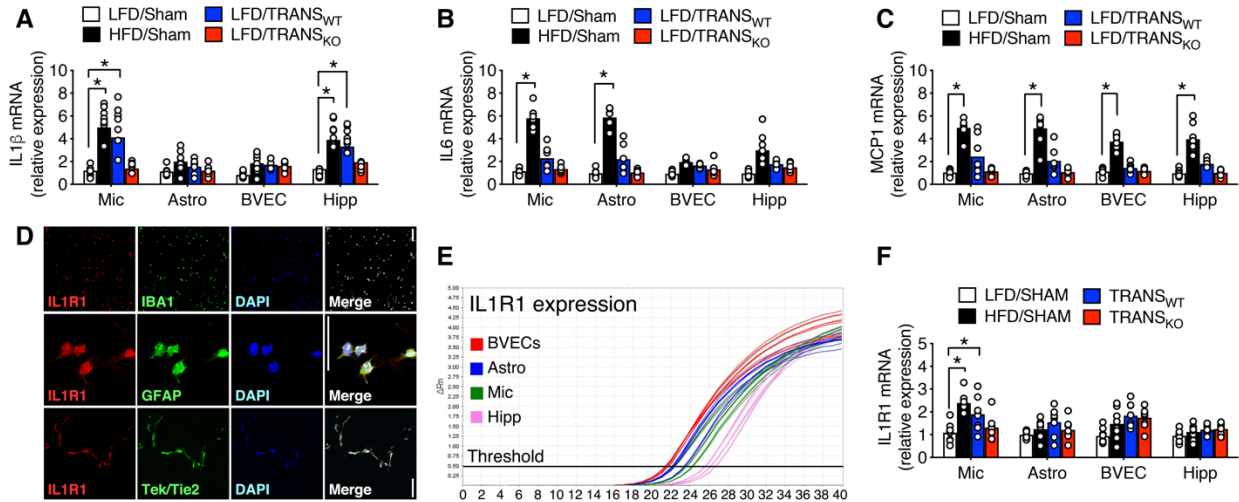
(B) No evidence of compensatory atrophy in resident adipose tissue. (C) qPCR analysis of IL1 β gene expression in resident (RES) and transplanted VAT (TRANS). (D) Depot-specific regulation of hippocampal IL1 β mRNA after transplantation of VAT or subcutaneous adipose tissue (SAT) from Wt mice with dietary obesity. (E) IL1 β gene expression in transplanted SAT did not differ from resident SAT in sham-operated mice.

For all graphs, bar height represents the mean and error bars represent SEM. Asterisk (*) denotes significant difference from LFD/SHAM and hashtags (#) indicate significant differences between TRANS_{WT} and TRANS_{KO}. The threshold for statistical significance was $p < 0.05$ determined by one-way ANOVA with Tukey's post hoc.

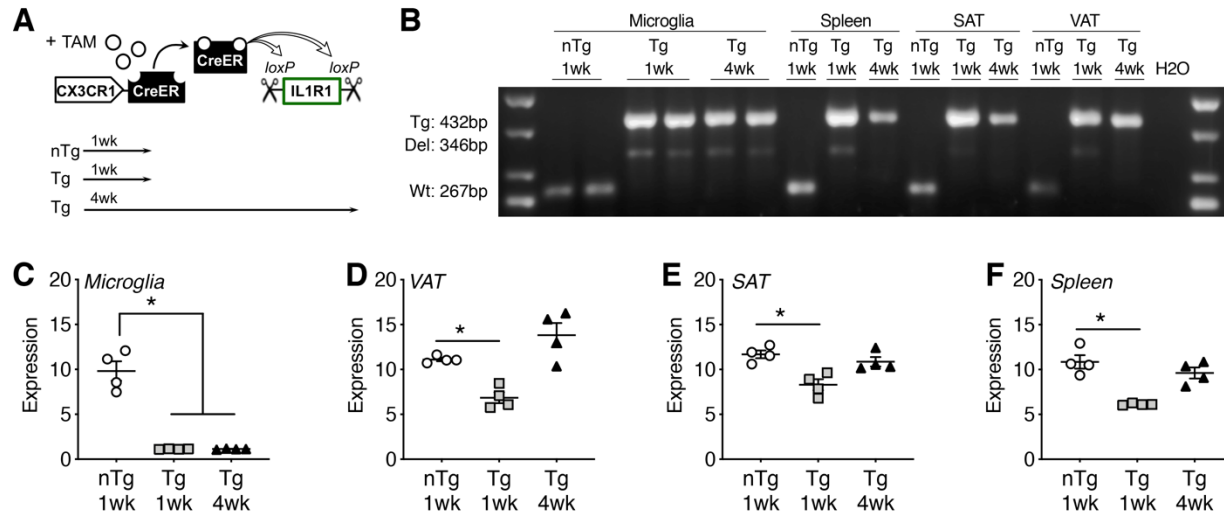


Supplemental Figure 3. Region-specific differences in CNS IL1 β following peripheral administration. (A) Top panel shows experimental design for analysis of hippocampal 6xHistidine-IL1 β after peripheral administration in LFD/SHAM, HFD/SHAM, TRANS_{WT}, and TRANS_{KO} mice. Bottom panel shows a representative western blot membrane probed with antibodies against 6xHis (~30kDa) and actin (42kDa). (B)

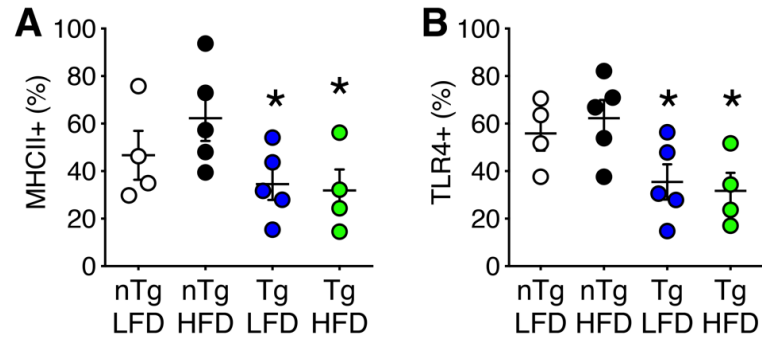
Increased levels of 6xHis-IL1 β in hippocampal lysates from HFD/SHAM and TRANS_{WT} mice (n=4). (C) No effect of diet or surgery on cortical levels of 6xHistidine-tagged IL1 β . (D) No effect of diet or surgery on 6xHis-IL1 β in hypothalamic lysates. (E) No detectable penetration of 6xHis-IL1 β in cerebellar lysates. (F) Increased penetration of peripheral IL1 β was associated with increased blood-brain barrier permeability to sodium fluorescein (NaFI) in HFD/SHAM mice, but not in transplant recipients. For all graphs, line height represents the mean and error bars represent SEM. Data were analyzed using one-way ANOVA with Tukey's post hoc (significance at $p < 0.05$).



Supplemental Figure 4. Cell type-specific regulation of gene expression with dietary obesity and VAT transplantation. (A) Analysis of IL1 β gene expression in primary microglia (Mic), astrocytes (Astro), brain vascular endothelial cells (BVECs), and whole-hippocampal cDNA revealed cell type-specific increases with dietary obesity or VAT transplantation. Increases in microglial and whole-hippocampal IL1 β gene expression were observed in TRANS_{WT} samples, but not in TRANS_{KO} samples. (B) Increases in interleukin-6 (IL6) gene expression were observed in primary microglia and astrocytes from HFD/SHAM mice, but were not recapitulated by VAT transplantation. (C) Dietary obesity increased the expression of MCP1/CCL2 mRNA in all cell types and in whole hippocampus. (D) All cell populations were immunoreactive for IL1R1 and phenotypic antigens (scale bar = 50 microns). (E) qPCR amplification curves show detectable levels of IL1R1 in all cell populations and in hippocampal cDNA. (F) VAT transplantation upregulates microglial IL1R1 expression via NLRP3. For all graphs, bar height represents the mean and error bars represent SEM. Asterisk (*) denotes statistical significance at $p < 0.05$ by one-way ANOVA with Tukey's post hoc.



Supplemental Figure 5. Selective recombination in forebrain microglia at 4wk post-induction in *CX3CR1^{creERT}/IL1R1^{fl/fl}* mice. (A) Schematic for analysis of IL1R1 deletion 1wk or 4wk post-tamoxifen. (B) Genomic DNA amplification with primers targeting the flox site (Tg), deleted region (Del), and the Wt allele (Wt) reveals selective deletion in primary microglia 4wk after tamoxifen. (C) Reduced expression of IL1R1 mRNA in FMCs 1wk and 4wk post-tamoxifen. (D-F) Transient reductions in IL1R1 gene expression 1wk after tamoxifen in VAT (D), SAT (E), and spleen (F). For all graphs, line height represents the mean and error bars represent SEM. Asterisk (*) denotes statistical significance at $p < 0.05$ by one-way ANOVA with Tukey's post hoc.



Supplemental Figure 6. Regulation of MHCII and TLR4 in CNS macrophages following IL1R1 deletion. (A) Deletion of IL1R1 in CX3CR1-expressing cells reduces MHCII expression in CD45hi/Ly6Chi/CD11b+ macrophages (n=4-5). (B) IL1R1 deletion reduces TLR4 expression in CNS macrophages (n=4-5). For all graphs, line height represents the mean and error bars represent SEM. Asterisk (*) denotes statistically significant effect of genotype at $p < 0.05$ by two-way ANOVA with Tukey's post hoc.